Journal of Applied Mechanical Engineering

Ueda and Kishimoto, J Appl Mech Eng 2016, 5:2
DOI: 10.4172/2168-9873.1000203

Research Article Open Access

Transient Thermoelectroelastic Response of a Functionally Graded Piezoelectric Material Strip with Two Parallel Cracks in Arbitrary Positions

Ueda S* and Kishimoto T

Department of Mechanical Engineering, Osaka Institute of Technology, Japan

Abstract

In this article, the problem of two parallel cracks in arbitrary positions of a functionally graded piezoelectric material (FGPM) strip is analyzed under transient thermal loading conditions. It is assumed that the thermoelectroelastic properties of the strip vary continuously along the thickness of the strip, and that the crack faces are supposed to be insulated thermally and electrically. By using both the Laplace transform and the Fourier transform, the thermal and electromechanical problems are reduced to two systems of singular integral equations. The singular integral equations are solved numerically, and a numerical method is then employed to obtain the time dependent solutions by way of a Laplace inversion technique. The intensity factors versus time for various geometric and material parameters are calculated and presented in graphical forms. Temperature change, the stress and electric displacement distributions in a transient state are also included.

Keywords: Thermo electroelasticity; Fracture mechanics; Functionally graded piezoelectric material; Arbitrary positions; Two parallel cracks; Integral transform; Transient response

Introduction

Piezoelectric materials widely have been used as sensors and actuators in smart or intelligent systems to sense thermally induced distortions and to adjust for adverse thermomechanical conditions [1,2]. The requirements of structural strength, reliability and lifetime of these structures call for a better understanding of the mechanics of fracture in piezoelectric materials under thermal loading.

Recently, functionally graded piezoelectric materials (FGPMs) have been developed to improve their reliability [3], and the electromechanical fracture of the FGPM under mechanical and electrical loadings has received much attention [4-6]. Thus, it is also important to investigate the fracture behavior of FGPMs under thermal load, and some interesting results have been reported [7-12].

While the fact that piezoelectric materials involve multiple cracks, most of the existing contributions are concerned with the fracture behavior of a single crack. Then some thermal fracture problems of homogeneous piezoelectric strips with two dimensional cracks, such as two coplanar cracks [13], two parallel cracks [14], parallel multi cracks [15] and a T-shaped crack [16], have been treated. Moreover, the over shooting phenomenon of intensity factors is observed in a piezoelectric plate under the thermal shock loading [17,18]. So, in this type of research, it is important to investigate the transient thermal fracture behavior of piezoelectric materials with multiple cracks. Although the present authors investigated the thermoelectromechanical interaction between two parallel axisymmetric cracks in an FGMP strip [19,20], one of the remaining problems that need to be fully understood is that of interaction between cracks in arbitrary positions of FGPMs under thermal shock loading.

In this study, the problem of two parallel cracks in arbitrary positions in a plate of an FGPM strip is analyzed under transient thermal loading conditions. It is assumed that the thermoelectroelastic properties of the strip vary continuously along the thickness of the strip, and that the crack faces are supposed to be insulated thermally and electrically [5,9]. By using both the Laplace and Fourier transform techniques [21,22], the thermal and electromechanical problems are reduced to two systems of singular integral equations. The singular integral equations are solved numerically [23], and a numerical method is employed to obtain time-dependent solutions by way of a Laplace inversion technique [24]. The intensity factors versus time for various geometric and material parameters are calculated.

Formulation of the Problem

Consider an infinite FGPM strip of thickness $h = h_1 + h_2$ containing two parallel through cracks of different length $2C_k$ (k = 1, 2) being spaced at distances $2d$ in the x-direction and $2h_0$ in the Z -direction as shown in Figure 1. The rectangular coordinates x, y and z are

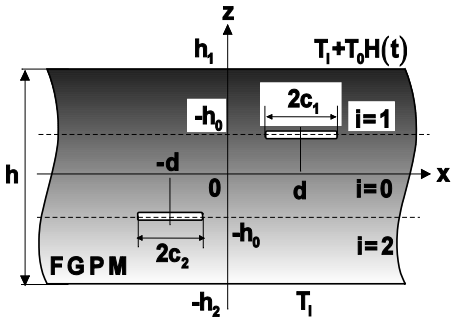

Figure 1: Geometry of the crack problem in a functionally graded piezoelectric strip.

***Corresponding author:** Ueda S, Department of Mechanical Engineering, Osaka Institute of Technology, 5-16-1 Omiya, Asahi-ku, Osaka, 535-8585, Japan, Tel: (816)6954-4263; E-mail: ueda@med.oit.ac.jp

Received February 09, 2016; **Accepted** March 09, 2016; **Published** March 13, 2016

Citation: Ueda S, Kishimoto T (2016) Transient Thermoelectroelastic Response of a Functionally Graded Piezoelectric Material Strip with Two Parallel Cracks in Arbitrary Positions. J Appl Mech Eng 5: 203. doi:10.4172/2168-9873.1000203

Copyright: © 2016 Ueda S, et al. This is an open-access article distributed under the terms of the Creative Commons Attribution License, which permits unrestricted use, distribution, and reproduction in any medium, provided the original author and source are credited.

coincident with the principal axes of the material. The piezoelectric strip is poled in the z-direction and is in the plane strain conditions perpendicular to the y -axis. It is assumed that initially the medium is at the uniform temperature T_1 and is suddenly subjected to a uniform temperature rise $T_0 H(t)$ along the boundary $Z = h_1$, where $H(t)$ is the Heaviside step function and t denotes time. The temperature along the boundary $Z = -h_2$ is maintained at T_1. The crack faces remain thermally and electrically insulated [5,9]. In the following, the subscripts x, y, z will be used to refer to the direction of coordinates.

The material properties, such as the elastic stiffness constants C_{kl}, the piezoelectric constants e_{kl}, the dielectric constants ε_{kk}, the stress-temperature coefficients λ_{kk}, the coefficients of heat conduction, K_x, K_z and the pyroelectric constant P_z are one-dimensionally dependent as

$$\left.\begin{aligned}(c_{kl}, e_{kl}, \varepsilon_{kk}) &= (c_{kl0}, e_{kl0}, \varepsilon_{kk0})\exp(\beta z)\\ (\lambda_{kk}, p_z) &= (\lambda_{kk0}, p_{z0})\exp[(\beta+\omega)z]\\ (\kappa_x, \kappa_z) &= (\kappa_{x0}, \kappa_{z0})\exp(\delta z)\end{aligned}\right\} \quad (1)$$

where β, ω and δ, are positive or negative constants, and the subscript 0 indicates the properties at the plane $Z = 0$. For some materials, the thermal diffusivity λ_0 indeed doesn't vary dramatically, and then λ_0 is assumed to be a constant.

The constitutive equations for the electroelastic fields are,

$$\left.\begin{aligned}\sigma_{xxi} &= c_{11}\frac{\partial u_{xi}}{\partial x} + c_{13}\frac{\partial u_{zi}}{\partial z} + e_{31}\frac{\partial \phi_i}{\partial z} - \lambda_{11}T_i\\ \sigma_{zzi} &= c_{13}\frac{\partial u_{xi}}{\partial x} + c_{33}\frac{\partial u_{zi}}{\partial z} + e_{33}\frac{\partial \phi_i}{\partial z} - \lambda_{33}T\\ \sigma_{zxi} &= c_{44}\left(\frac{\partial u_{xi}}{\partial z} + \frac{\partial u_{zi}}{\partial x}\right) + e_{15}\frac{\partial \phi_i}{\partial x}\end{aligned}\right\} \quad (i = 0,1,2) \quad (2)$$

where $T_i \equiv T_i(x,z,t)$ is the temperature, $\varphi_i \equiv \varphi_i(x,z,t)$ is the electric potential, $u_{xi} \equiv u_{xi}(_{zxi})$, $u_{zi} \equiv u_{zi}(x,z,t)$, are the displacement components, $\sigma_{xxi} \equiv \sigma_{xxi}(x,z,t)$, $\sigma_{zzi} \equiv \sigma_{zzi}(x,z,t)$, $_{zxi} \equiv \sigma_{zxi}(x,z,t)$ $(i = 0,1, 2)$ are the stress components. The subscript i = 0,1,2 denotes the thermoelectroelastic fields in $-h_0 \le Z \le h_0$, $h_0 \le Z \le h_1$, $-h_2 \le Z \le -h_1$ respectively. For the electric field, the constitutive relations are

$$\left.\begin{aligned}D_{xi} &= e_{15}\left(\frac{\partial u_{xi}}{\partial z} + \frac{\partial u_{zi}}{\partial x}\right) - \varepsilon_{11}\frac{\partial \phi_i}{\partial x}\\ D_{zi} &= e_{31}\frac{\partial u_{xi}}{\partial x} + e_{33}\frac{\partial u_{zi}}{\partial z} - \varepsilon_{33}\frac{\partial \phi_i}{\partial z} + p_z T\end{aligned}\right\} \quad (i = 0,1,2) \quad (3)$$

Where $D_{xi} \equiv D_{xi}(x,z,t)$, $D_{zi} \equiv D_{zi}(x,z,t)$ $(i = 0,1,2)$ are the electric displacement components.

The temperature is assumed to satisfy the Fourier heat conduction equations:

$$\kappa^2\frac{\partial^2 T_i}{\partial x^2} + \frac{\partial^2 T_i}{\partial z^2} + \delta\frac{\partial T_i}{\partial z} = \frac{1}{\lambda_0}\frac{\partial T_i}{\partial t} \quad (i = 0,1,2) \quad (4)$$

where $\kappa^2 = \kappa_x/\kappa_z$. The equations of equilibrium and electrostatics are,

$$\left.\begin{aligned}&c_{110}\frac{\partial^2 u_{xi}}{\partial x^2} + c_{440}\frac{\partial^2 u_{xi}}{\partial z^2} + (c_{130}+c_{440})\frac{\partial^2 u_{zi}}{\partial x \partial z} + (e_{310}+e_{150})\frac{\partial^2 \phi_i}{\partial x \partial z}\\ &+\beta\left[c_{440}\left(\frac{\partial u_{xi}}{\partial z} + \frac{\partial u_{zi}}{\partial x}\right) + e_{150}\frac{\partial \phi_i}{\partial z}\right] = \lambda_{110}\exp(\omega z)\frac{\partial T_i}{\partial x}\\ &c_{440}\frac{\partial^2 u_{zi}}{\partial x^2} + c_{330}\frac{\partial^2 u_{zi}}{\partial z^2} + (c_{130}+c_{440})\frac{\partial^2 u_{xi}}{\partial x \partial z} + e_{150}\frac{\partial^2 \phi_i}{\partial x^2} + e_{330}\frac{\partial^2 \phi_i}{\partial z^2}\\ &+\beta\left(c_{130}\frac{\partial u_{xi}}{\partial x} + c_{330}\frac{\partial u_{zi}}{\partial z} + e_{330}\frac{\partial \phi_i}{\partial z}\right) = \lambda_{330}\exp(\omega z)\left[\frac{\partial T_i}{\partial z} + (\beta+\omega)T_i\right]\\ &e_{150}\frac{\partial^2 u_{zi}}{\partial x^2} + e_{330}\frac{\partial^2 u_{zi}}{\partial z^2} + (e_{150}+e_{310})\frac{\partial^2 u_{xi}}{\partial x \partial z} - \varepsilon_{110}\frac{\partial^2 \phi_i}{\partial x^2} - \varepsilon_{330}\frac{\partial^2 \phi_i}{\partial z^2}\\ &+\beta\left(e_{310}\frac{\partial u_{xi}}{\partial x} + e_{330}\frac{\partial u_{zi}}{\partial z} - \varepsilon_{330}\frac{\partial \phi_i}{\partial z}\right) = -p_{z0}\exp(\omega z)\left[\frac{\partial T_i}{\partial z} + (\beta+\omega)T_i\right]\end{aligned}\right\} (i = 0,1,2) \quad (5)$$

The initial and boundary conditions for the temperature field can be written as

$$T_i(x,z,0) = T_1 \quad (i = 0,1,2) \quad (6)$$

$$\left.\begin{aligned}\frac{\partial T_0(x,\theta_{0i},t)}{\partial z} &= 0 \qquad (a_i < x < b_i)\\ T_0(x,\theta_{0i},t) &= T_i(x,\theta_{0i},t) \quad (-\infty < x \le a_i, b_i \le x < \infty)\end{aligned}\right\} \quad (i = 1,2) \quad (7)$$

$$\left.\begin{aligned}\frac{\partial T_0(x,\theta_{0i},t)}{\partial z} &= \frac{\partial T_i(x,\theta_{0i},t)}{\partial z} \qquad (-\infty < x < \infty)\\ T_i(x,\theta_{1i},t) &= \begin{Bmatrix}T_1 + T_0 H(t) & (i=1)\\ T_1 & (i=2)\end{Bmatrix} \quad (-\infty < x < \infty)\end{aligned}\right\} \quad (i = 1,2) \quad (8)$$

If the electrically impermeable boundary is chosen as an idealized crack face electric boundary condition [9,25], the boundary conditions of this problem can be written as

$$\left.\begin{aligned}\sigma_{zz0}(x,\theta_{0i},t) &= 0 \qquad (a_i < x < b_i)\\ u_{z0}(x,\theta_{0i},t) &= u_{zi}(x,\theta_{0i},t) \quad (-\infty < x \le a_i, b_i \le x < \infty)\end{aligned}\right\} \quad (i = 1,2) \quad (9)$$

$$\left.\begin{aligned}\sigma_{zx0}(x,\theta_{0i},t) &= 0 \qquad (a_i < x < b_i)\\ u_{x0}(x,\theta_{0i},t) &= u_{xi}(x,\theta_{0i},t) \quad (-\infty < x \le a_i, b_i \le x < \infty)\end{aligned}\right\} \quad (i = 1,2) \quad (10)$$

$$\left.\begin{aligned}D_{z0}(x,\theta_{0i},t) &= 0 \qquad (a_i < x < b_i)\\ \phi_0(x,\theta_{0i},t) &= \phi_i(x,\theta_{0i},t) \quad (-\infty < x \le a_i, b_i \le x < \infty)\end{aligned}\right\} \quad (i = 1,2) \quad (11)$$

$$\left.\begin{aligned}\sigma_{zz0}(x,\theta_{0i},t) &= \sigma_{zzi}(x,\theta_{0i},t) \quad (-\infty < x < \infty)\\ \sigma_{zx0}(x,\theta_{0i},t) &= \sigma_{zxi}(x,\theta_{0i},t) \quad (-\infty < x < \infty)\\ D_{z0}(x,\theta_{0i},t) &= D_{zi}(x,\theta_{0i},t) \quad (-\infty < x < \infty)\end{aligned}\right\} \quad (i = 1,2) \quad (12)$$

$$\left.\begin{aligned}\sigma_{zzi}(x,\theta_{1i},t) &= 0 \quad (-\infty < x < \infty)\\ \sigma_{zxi}(x,\theta_{1i},t) &= 0 \quad (-\infty < x < \infty)\\ D_{zi}(x,\theta_{1i},t) &= 0 \quad (-\infty < x < \infty)\end{aligned}\right\} \quad (i = 1,2) \quad (13)$$

In Eqs. (7)-(13), θ_{0i}, θ_{1i}, α_i and b_i $(i = 1,2)$ are given by

$$(\theta_{0i}, \theta_{1i}, a_i, b_i) = \begin{Bmatrix}(h_0, h_1, d-c_1, d+c_1) & (i=1)\\ (-h_0, -h_2, -d-c_2, -d+c_2) & (i=2)\end{Bmatrix} \quad (14)$$

Temperature Field

For the problem considered here, it is convenient to represent the temperature $T_i(x,z,t)$ $(i = 0,1,2)$ as the sum of the uniform temperature T_1 and two functions.

$$T_i(x,z,t) = T_1 + T^{(1)}(z,t) + T_i^{(2)}(x,z,t) \quad (i = 0,1,2) \quad (15)$$

where the non-disturbed temperature $T^{(1)} \equiv T^{(1)}(z,t)$ satisfies the following equation accompanied by initial and boundary conditions:

$$\frac{\partial^2 T^{(1)}}{\partial z^2}+\delta\frac{\partial T^{(1)}}{\partial z}=\frac{1}{\lambda_0}\frac{\partial T^{(1)}}{\partial t} \tag{16}$$

$$T^{(1)}(z,0)=0 \tag{17}$$

$$\left.\begin{aligned} T^{(1)}(h_1,t)&=T_0H(t)\\ T^{(1)}(-h_2,t)&=0\end{aligned}\right\} \tag{18}$$

and the disturbed temperatures $T_i^{(2)}\equiv T_i^{(2)}(x,z,t)$ $(i=0,1,2)$ are subjected to the relations:

$$\kappa^2\frac{\partial^2 T_i^{(2)}}{\partial x^2}+\frac{\partial^2 T_i^{(2)}}{\partial z^2}+\delta\frac{\partial T_i^{(2)}}{\partial z}=\frac{1}{\lambda_0}\frac{\partial T_i^{(2)}}{\partial t}\quad (i=0,1,2) \tag{19}$$

$$T_i^{(2)}(x,z,0)=0\quad (i=0,1,2) \tag{20}$$

$$\left.\begin{aligned} \frac{\partial T_0^{(2)}(x,\theta_{0i},t)}{\partial z}&=-\frac{\partial T^{(1)}(\theta_{0i},t)}{\partial z} && (a_i<x<b_i)\\ T_0^{(2)}(x,\theta_{0i},t)&=T_i^{(2)}(x,\theta_{0i},t) && (-\infty<x\le a_i,b_i\le x<\infty)\end{aligned}\right\}\ (i=1,2) \tag{21}$$

$$\left.\begin{aligned} \frac{\partial T_0^{(2)}(x,\theta_{0i},t)}{\partial z}&=\frac{\partial T_i^{(2)}(x,\theta_{0i},t)}{\partial z} && (-\infty<x<\infty)\\ T_i^{(2)}(x,\theta_{1i},t)&=0 && (-\infty<x<\infty)\end{aligned}\right\}\ (i=1,2) \tag{22}$$

Define a Laplace transform pair by

$$f^*(p)=\int_0^\infty f(t)\exp(-pt)dt,\quad f(t)=\frac{1}{2\pi i}\int_{Br}f^*(p)\exp(pt)dp \tag{23}$$

where *Br* denotes the Bromwich path in pertinent complex planes, and applying the Laplace transform, it is easy to find from Eqs. (16)-(18) that

$$T^{(1)*}(z,p)=\frac{T_0}{p[1-\exp(-2\mu_0 h)]}\{\exp[\mu_2(h_1-z)]-\exp[-2\mu_0 h+\mu_1(h_1-z)]\} \tag{24}$$

with

$$\left.\begin{aligned} \mu_0&=\left(\frac{\delta^2}{4}+\frac{p}{\lambda_0}\right)^{1/2}\\ \mu_1&=\frac{\delta}{2}+\mu_0,\quad \mu_2=\frac{\delta}{2}-\mu_0\end{aligned}\right\} \tag{25}$$

In the following, the superscript * is used to refer to the physical quantities in the Laplace transform plane.

The general solutions of the governing Eq. (19) can be obtained by using the Laplace-Fourier integral transform techniques [21]:

$$T_i^{(2)*}(x,z,p)=\frac{1}{2\pi}\sum_{j=1}^{2}\int_{-\infty}^{\infty}D_{ij}(s,p)\exp(|s|\tau_{ij}z)\exp(-isx)ds\quad (i=0,1,2) \tag{26}$$

In the above expressions, $D_{ij}(s,p)(i=0,1,2,\ j=1,2)$ are unknown functions to be solved and

τ_{ij} $\tau_{ij}(s,p)$ $(i=0,1,2, j=1,2)$ are defined as

$$\left.\begin{aligned} \tau_{i1}(s,p)&=-\tau-\frac{\delta}{2|s|},\quad \tau_{i2}(s,p)=\tau-\frac{\delta}{2|s|}\\ \tau\equiv\tau(s,p)&=\left[\kappa^2+\left(\frac{\delta}{2|s|}\right)^2+\frac{p}{\lambda_0 s^2}\right]^{1/2}\end{aligned}\right\}\quad (i=0,1,2) \tag{27}$$

The problem may be reduced to a system of singular integral equations by defining the following new unknown functions $G_{k0}(x,p)$ $(k=1,2)$ [22]:

$$G_{k0}(x,p)=\left\{\begin{matrix}\frac{\partial}{\partial x}\left[T_0^{(2)*}(x,\theta_{0k},p)-T_k^{(2)*}(x,\theta_{0k},p)\right] & (a_k<x<b_k)\\ 0 & (-\infty<x\le a_k,b_k\le x<\infty)\end{matrix}\right\}\quad (k=1,2) \tag{28}$$

Making use of the first boundary conditions (21) with Eqs. (22), we have the following system of the singular integral equations for the determination of the unknown functions $G_{k0}(\xi,p)(k=1,2)$:

$$\frac{\kappa}{2\pi}\int_{a_1}^{b_1}\left[\frac{1}{\xi-x}+M_{011}(\xi,x,p)\right]G_{10}(\xi,p)d\xi$$

$$-\int_{a_2}^{b_2}M_{012}(\xi,x,p)G_{20}(\xi,p)d\xi=\frac{d}{dz}T^{(1)*}(h_0,p)\quad (a_1<x<b_1) \tag{29}$$

$$\frac{\kappa}{2\pi}\int_{a_1}^{b_1}M_{021}(\xi,x,p)G_{10}(\xi,p)d\xi$$

$$-\int_{a_2}^{b_2}\left[\frac{1}{\xi-x}+M_{022}(\xi,x,p)\right]G_{20}(\xi,p)d\xi=\frac{d}{dz}T^{(1)*}(-h_0,p)\quad (a_2<x<b_2) \tag{30}$$

In Eqs. (29) and (30), the kernel functions $M_{0nk}(\xi,x,p)(n,k=1,2)$ are given by

$$\left.\begin{aligned} M_{011}(\xi,x,p)&=\int_0^\infty\left\{\left(\frac{\tau_{02}\rho_1}{\kappa\tau\rho_0}-1\right)-\frac{\tau_{01}\rho_1}{\kappa\tau\rho_0}\exp[-2s\tau(h_2+h_0)]\right\}\sin[s(\xi-x)]ds\\ M_{012}(\xi,x,p)&=-\int_0^\infty\frac{\rho_2}{\kappa\tau\rho_0}\{\tau_{01}\exp(2s\tau_{01}h_0)\\ &\quad-\tau_{02}\exp[-s(2\tau h_1-\tau_{01}h_0-\tau_{02}h_0)]\}\sin[s(\xi-x)]ds\\ M_{021}(\xi,x,p)&=\int_0^\infty\frac{\rho_2}{\kappa\tau\rho_0}\{\tau_{02}\exp(2s\tau_{02}h_0)\\ &\quad-\tau_{01}\exp[-s(2\tau h_2-\tau_{02}h_0-\tau_{01}h_0)]\}\sin[s(\xi-x)]ds\\ M_{022}(\xi,x,p)&=-\int_0^\infty\left\{\left(\frac{\tau_{01}\rho_2}{\kappa\tau\rho_0}-1\right)-\frac{\tau_{02}\rho_2}{\kappa\tau\rho_0}\exp[-2s\tau(h_1+h_0)]\right\}\sin[s(\xi-x)]ds\end{aligned}\right\} \tag{31}$$

Where

$$\left.\begin{aligned} \rho_1&\equiv\rho_1(s,p)=-\tau_{11}+\tau_{12}\exp[-2s\tau(h_1-h_0)]\\ \rho_2&\equiv\rho_2(s,p)=\tau_{22}-\tau_{21}\exp[-2s\tau(h_2-h_0)]\\ \rho_0&\equiv\rho_0(s,p)=1-\exp(-2s\tau h)\end{aligned}\right\} \tag{32}$$

It is noted that the kernel functions $M_{011}(,x,p)$, $M_{022}(\xi,x,p)$ are semi-infinite integrals which have rather slow rate of convergence. To simplify the numerical analysis, the kernels are evaluated as follows:

$$M_{011}(\xi,x,p)=M_{011}^{\infty}(\xi,x,p)+\int_0^\infty\frac{\tau}{\kappa\rho_0}\{\exp[-2|s|\tau(h_1-h_0)]+\exp[-2|s|\tau(h_2+h_0)]$$

$$+2\exp[-2|s|\tau(h_1+h_2)]\}\sin[s(\xi-x)]ds$$

$$+\int_0^\infty\frac{\delta}{\kappa\rho_0|s|}\{\exp[-2|s|\tau(h_2+h_0)]+\exp[-2|s|\tau(h_1-h_0)]\}\sin[s(\xi-x)]ds$$

$$-\int_0^\infty\frac{1}{\kappa\tau\rho_0}\left(\frac{\delta}{2|s|}\right)^2\{1+\exp(-2|s|\tau h)-\exp[-2|s|\tau(h_2+h_0)]$$

$$-\exp[-2|s|\tau(h_1-h_0)]\}\sin[s(\xi-x)]ds \tag{33}$$

$$M_{022}(\xi,x,p)=M_{022}^{\infty}(\xi,x,p)+\int_0^\infty\frac{\tau}{\kappa\rho_0}\{\exp[-2|s|\tau(h_1+h_0)]+\exp[-2|s|\tau(h_2-h_0)]$$

$$+2\exp[-2|s|\tau(h_1+h_2)]\}\sin[s(\xi-x)]ds$$

$$+\int_0^\infty\frac{\delta}{\kappa\rho_0|s|}\{\exp[-2|s|\tau(h_2-h_0)]-\exp[-2|s|\tau(h_1+h_0)]\}\sin[s(\xi-x)]ds$$

$$-\int_0^\infty\frac{1}{\kappa\tau\rho_0}\left(\frac{\delta}{2|s|}\right)^2\{1+\exp(-2|s|\tau h)-\exp[-2|s|\tau(h_1+h_0)]$$

$$-\exp\left[-2|s|\tau(h_2-h_0)\right]\Big\}\sin\left[s(\xi-x)\right]ds \tag{34}$$

Where the kernel functions $M^{\infty}_{011}(\xi,x,p)$, $M^{\infty}_{022}(\xi,x,p)$ are given in Appendix A.

The system of the singular integral equations (29) and (30) is to be solved with the following subsidiary conditions obtained from the second boundary conditions of Eqs. (21).

$$\int_{a_k}^{b_k} G_{k0}(\xi,p)d\xi = 0 \quad (k=1,2) \tag{35}$$

The solution procedure of the system of the singular integral equations will be explained lately.

Once $G_{k0}(\xi, p)(k = 1,2)$ are obtained from Eqs. (29), (30) and (35), the temperature field in the Laplace transform plane can be easily calculated as follows:

$$T_i^{(2)*}(x,z,p) = -\frac{1}{\pi}\sum_{j=1}^{2}\sum_{k=1}^{2}\int_0^{\infty}\frac{1}{s}R_{ijk}\exp\left[s(\tau_{ij}z+\tau h_{ij})\right]ds$$

$$\times\int_{a_k}^{b_k} G_{k0}(\xi,p)\sin\left[s(\xi-x)\right]d\xi \quad (i=0,1,2) \tag{36}$$

where the functions $R_{ijk} \equiv R_{ijk}(s,p)$ are given in Appendix B, and constants $h_{ij}(i = 0,1,2, j,k = 1,2)$ are

$$\left.\begin{aligned} &h_{01}=h_{02}=-h_0, \quad h_{11}=h_{22}=h_0\\ &h_{12}=-2h_1+h_0, \quad h_{21}=-2h_2+h_0 \end{aligned}\right\} \tag{37}$$

The temperature fields $T^{(1)}(z,t)$ and $T_i^{(2)}(x,z,t)$ $(i = 0,1,2)$ in the time-domain can be obtained from $T^{(1)*}(z,p)$ and $T^{(2)*}(x,z,p)(i = 0,1,2)$ by use of the numerical inversion technique of the Laplace transform [24].

Thermally Induced Singular Elastic and Electric Fields

The non-disturbed temperature field $T^{(1)*}(z,p)$ given by Eq. (24) does not induce the stress and electric displacement components affecting the singular field. Thus, we consider the elastic and electric fields due to the disturbed temperature distribution $T_i^{(2)*}(x,z,p)(i=0,1,2)$ only in this section. It is convenient to represent the solutions $u_{zi}^*(x,z,p)$, $u_{xi}^*(x,z,p)$ and $\phi_i^*(x,z,p)(i=0,1,2)$ in the Laplace transform plane as the sum of two functions, respectively.

$$\left.\begin{aligned} u_{zi}^*(x,z,p) &= u_{zi}^{(1)*}(x,z,p)+u_{zi}^{(2)*}(x,z,p)\\ u_{xi}^*(x,z,p) &= u_{xi}^{(1)*}(x,z,p)+u_{xi}^{(2)*}(x,z,p)\\ \phi_i^*(x,z,p) &= \phi_i^{(1)*}(x,z,p)+\phi_i^{(2)*}(x,z,p) \end{aligned}\right\} \quad (i=0,1,2) \tag{38}$$

where $u_{zi}^{(1)*}(x,z,p)$, $u_{xi}^{(1)*}(x,z,p)$, $\phi_i^{(1)*}(x,z,p)$ are the particular solutions of Eq. (5) replaced $T_i^*(x,z,p)$ by $T_i^{(2)*}(x,z,p)$, and $u_{zi}^{(2)*}(x,z,p)$, $u_{xi}^{(2)*}(x,z,p)$, $\phi_i^{(2)*}(x,z,p)$ are the general solutions of homogeneous equations obtained by setting $T_i^*(x,z,p)=0\,(i=0,1,2)$ in Eq. (5). In the following, the superscripts (1) and (2) indicate the particular and general solutions of Eq. (5). Substituting Eq. (38) into Eqs. (2) and (3), one can obtain the stress $\sigma_{xxi}^*(x,z,p)$, $\sigma_{zzi}^*(x,z,p)$, $\sigma_{zxi}^*(x,z,p)$ and electric displacement $D_{xi}^*(x,z,p)$, $D_{zi}^*(x,z,p)$ $(i=0,1,2)$ expressions in the Laplace transform plane.

Using the displacement potential function method and the Fourier integral transform techniques [21], the particular and general solutions can be obtained as follows:

$$\left.\begin{aligned} u_{zi}^{(1)*}(x,z,p) &= \frac{1}{2\pi}\sum_{j=1}^{2}\int_{-\infty}^{\infty}\frac{1}{s|s|}p_{4ij}^{(1)}F_{ij}(s,p)\exp\left[|s|(f_{ij}z+\tau h_{ij})\right]\exp(-\mathrm{i}sx)ds\\ u_{xi}^{(1)*}(x,z,p) &= \frac{1}{2\pi}\sum_{j=1}^{2}\int_{-\infty}^{\infty}\frac{1}{s^2}p_{5ij}^{(1)}F_{ij}(s,p)\exp\left[|s|(f_{ij}z+\tau h_{ij})\right]\exp(-\mathrm{i}sx)ds\\ \phi_i^{(1)*}(x,z,p) &= -\frac{1}{2\pi}\sum_{j=1}^{2}\int_{-\infty}^{\infty}\frac{1}{s|s|}p_{6ij}^{(1)}F_{ij}(s,p)\exp\left[|s|(f_{ij}z+\tau h_{ij})\right]\exp(-\mathrm{i}sx)ds \end{aligned}\right\} (i=0,1,2) \tag{39}$$

$$\left.\begin{aligned} u_{zi}^{(2)*}(x,z,p) &= \frac{\mathrm{i}}{2\pi}\sum_{j=1}^{6}\int_{-\infty}^{\infty}p_{4ij}^{(2)}A_{ij}(s,p)\exp(|s|\gamma_{ij}z)\exp(-\mathrm{i}sx)ds\\ u_{xi}^{(2)*}(x,z,p) &= \frac{\mathrm{i}}{2\pi}\sum_{j=1}^{6}\int_{-\infty}^{\infty}\frac{|s|}{s}p_{5ij}^{(2)}A_{ij}(s,p)\exp(|s|\gamma_{ij}z)\exp(-\mathrm{i}sx)ds\\ \phi_i^{(2)*}(x,z,p) &= -\frac{\mathrm{i}}{2\pi}\sum_{j=1}^{6}\int_{-\infty}^{\infty}p_{6ij}^{(2)}A_{ij}(s,p)\exp(|s|\gamma_{ij}z)\exp(-\mathrm{i}sx)ds \end{aligned}\right\} (i=0,1,2) \tag{40}$$

where $A_{ij}(s,p)$ are the unknown functions to be solved. The functions $p_{mij}^{(1)} \equiv p_{mij}^{(1)}(s,p)$, $f_{ij} \equiv f_{ij}(s,p)$ $(m = 4,5,6,\ i = 0,1,2,\ j = 1,2)$ are given in Appendix C, and $p_{mij}^{(2)} \equiv p_{mij}^{(2)}(s)$, $\gamma ij \equiv \gamma ij\ (S)$ $(m = 4,5,6,\ i = 0,1,2,\ j = 1,2,\ldots,6)$ are given in Appendix A of the previous paper [19]. The functions $F_{ij}(s,p)$ $(i = 0,1,2,\ j = 1,2)$ are

$$F_{ij}(s,p) = \sum_{k=1}^{2}R_{ijk}\int_{a_k}^{b_k}G_{k0}(\xi,p)\exp(\mathrm{i}s\xi)d\xi \quad (i=0,1,2,\ j=1,2) \tag{41}$$

Similar to the temperature analysis, the problem may be reduced to a system of singular integral equations by defining the following new unknown functions $G_{km}(x,p)$ (k = 1, 2, m = 1, 2, 3) [21]:

$$G_{k1}(x,p) = \left\{\begin{array}{ll}\dfrac{\partial}{\partial x}\left[u_{z0}^*(x,\theta_{0k},p)-u_{zk}^*(x,\theta_{0k},p)\right] & (a_k<x<b_k)\\ 0 & (-\infty<x\le a_k,b_k\le x<\infty)\end{array}\right\} \quad (k=1,2) \tag{42}$$

$$G_{k2}(x,p) = \left\{\begin{array}{ll}\dfrac{\partial}{\partial x}\left[u_{x0}^*(x,\theta_{0k},p)-u_{xk}^*(x,\theta_{0k},p)\right] & (a_k<x<b_k)\\ 0 & (-\infty<x\le a_k,b_k\le x<\infty)\end{array}\right\} \quad (k=1,2) \tag{43}$$

$$G_{k3}(x,p) = \left\{\begin{array}{ll}-\dfrac{\partial}{\partial x}\left[\phi_0^*(x,\theta_{0k},p)-\phi_k^*(x,\theta_{0k},p)\right] & (a_k<x<b_k)\\ 0 & (-\infty<x\le a_k,b_k\le x<\infty)\end{array}\right\} \quad (k=1,2) \tag{44}$$

Making use of the first boundary conditions (9)-(11) with Eqs. (12) and (13), we have the following system of six singular integral equations for the determination of the unknown functions $G_{km}(\xi, p)$ (k = 1, 2, m = 1, 2, 3)

$$\int_{a_1}^{b_1}\left\{\left[\frac{Z_{1111}^{(1)\infty}}{\xi-x}+M_{111}^{(1)}(\xi,x)\right]G_{11}(\xi,p)+M_{112}^{(1)}(\xi,x)G_{12}(\xi,p)+\left[\frac{Z_{1131}^{(1)\infty}}{\xi-x}+M_{113}^{(1)}(\xi,x)\right]G_{13}(\xi,p)\right\}d\xi$$

$$+\int_{a_2}^{b_2}\sum_{m=1}^{3}M_{12m}^{(1)}(\xi,x)G_{2m}(\xi,p)d\xi = \pi\sigma_{zz0}^{T*}(x,h_0,p) \quad (a_1<x<b_1) \tag{45}$$

$$\int_{a_1}^{b_1}\left\{M_{211}^{(1)}(\xi,x)G_{11}(\xi,p)+\left[\frac{Z_{2121}^{(1)\infty}}{\xi-x}+M_{212}^{(1)}(\xi,x)\right]G_{12}(\xi,p)+M_{213}^{(1)}(\xi,x)G_{13}(\xi,p)\right\}d\xi$$

$$+\int_{a_2}^{b_2}\sum_{m=1}^{3}M_{22m}^{(1)}(\xi,x)G_{2m}(\xi,p)d\xi = \pi\sigma_{zx0}^{T*}(x,h_0,p) \quad (a_1<x<b_1) \tag{46}$$

$$\int_{a_1}^{b_1}\left\{\left[\frac{Z_{3111}^{(1)\infty}}{\xi-x}+M_{311}^{(1)}(\xi,x)\right]G_{11}(\xi,p)+M_{312}^{(1)}(\xi,x)G_{12}(\xi,p)+\left[\frac{Z_{3131}^{(1)\infty}}{\xi-x}+M_{313}^{(1)}(\xi,x)\right]G_{13}(\xi,p)\right\}d\xi$$

$$+\int_{a_2}^{b_2}\sum_{m=1}^{3}M_{32m}^{(1)}(\xi,x)G_{2m}(\xi,p)d\xi = \pi D_{z0}^{T*}(x,h_0,p) \quad (a_1<x<b_1) \tag{47}$$

$$\int_{a_2}^{b_2}\left\{\left[\frac{Z_{1211}^{(2)\infty}}{\xi-x}+M_{121}^{(2)}(\xi,x)\right]G_{21}(\xi,p)+M_{122}^{(2)}(\xi,x)G_{22}(\xi,p)+\left[\frac{Z_{1231}^{(2)\infty}}{\xi-x}+M_{123}^{(2)}(\xi,x)\right]G_{23}(\xi,p)\right\}d\xi$$

$$+\int_{a_1}^{b_1}\sum_{m=1}^{3}M_{11m}^{(2)}(\xi,x)G_{1m}(\xi,p)d\xi = \pi\sigma_{zz0}^{T*}(x,-h_0,p) \quad (a_2<x<b_2) \tag{48}$$

$$\int_{a_2}^{b_2}\left\{M_{221}^{(2)}(\xi,x)G_{21}(\xi,p)+\left[\frac{Z_{2221}^{(2)\infty}}{\xi-x}+M_{222}^{(2)}(\xi,x)\right]G_{22}(\xi,p)+M_{223}^{(2)}(\xi,x)G_{23}(\xi,p)\right\}d\xi$$

$$+\int_{a_1}^{b_1}\sum_{m=1}^{3}M_{21m}^{(2)}(\xi,x)G_{1m}(\xi,p)d\xi = \pi\sigma_{zx0}^{T*}(x,-h_0,p) \quad (a_2<x<b_2) \tag{49}$$

$$\int_{a_2}^{b_2}\left\{\left[\frac{Z_{3211}^{(2)\infty}}{\xi-x}+M_{321}^{(2)}(\xi,x)\right]G_{21}(\xi,p)+M_{322}^{(2)}(\xi,x)G_{22}(\xi,p)+\left[\frac{Z_{3231}^{(2)\infty}}{\xi-x}+M_{323}^{(2)}(\xi,x)\right]G_{23}(\xi,p)\right\}d\xi$$

$$+\int_{a_1}^{b_1}\sum_{m=1}^{3}M_{31m}^{(2)}(\xi,x)G_{1m}(\xi,p)d\xi=\pi D_{z0}^{T*}(x,-h_0,p)\quad(a_2<x<b_2)\tag{50}$$

In the above equations, the kernel functions $M_{jkm}^{(n)}(\xi,x)(n,k=1,2,j,m=1,2,3)$ are given by

$$M_{jkm}^{(n)}(\xi,x)=\left\{\begin{array}{l}\left\{\begin{array}{l}\int_{-\infty}^{\infty}\sum_{l=1}^{2}\left[Z_{jkml}^{(n)}(s)-Z_{jkml}^{(n)\infty}\right]\sin\left[s(\xi-x)\right]ds\quad(m=1,3)\\-\int_{-\infty}^{\infty}\sum_{l=1}^{2}\left[Z_{jkml}^{(n)}(s)-Z_{jkml}^{(n)\infty}\right]\cos\left[s(\xi-x)\right]ds\quad(m=2)\end{array}\right\}\ (j=1,3)\\\left\{\begin{array}{l}\int_{-\infty}^{\infty}\sum_{l=1}^{2}\left[Z_{jkml}^{(n)}(s)-Z_{jkml}^{(n)\infty}\right]\cos\left[s(\xi-x)\right]ds\quad(m=1,3)\\\int_{-\infty}^{\infty}\sum_{l=1}^{2}\left[Z_{jkml}^{(n)}(s)-Z_{jkml}^{(n)\infty}\right]\sin\left[s(\xi-x)\right]ds\quad(m=2)\end{array}\right\}\ (j=2)\end{array}\right\}(n,k=1,2)\tag{51}$$

where the functions $Z_{jkml}^{(n)}(s)$ and the constants $Z_{jkml}^{(n)\infty}(n,k,l=1,2,j,m=1,2,3)$ are given in Appendix D. The functions $\sigma_{zz0}^{T*}(x,\pm h_0,p)$, $\sigma_{zx0}^{T*}(x,\pm h_0,p)$ and $D_{z0}^{T*}(x,\pm h_0,p)$, which correspond to the stress and electric displacement components induced by the disturbed temperatures $T_i^{(2)*}(x,z,p)(i=0,1,2)$ on the $z=\pm h_0$ planes in the absence of the crack, are obtained as follows:

$$\begin{aligned}\sigma_{zz0}^{T*}(x,\pm h_0,p)&=\lim_{z\to\pm h_0}\frac{1}{2\pi}\sum_{j=1}^{3}\int_{-\infty}^{\infty}|s|\,p_{10j}^{(2)}d_{0j}^{T}(s,p)\exp\left[|s|\gamma_{oj}(h_0+z)\right]\exp(-isx)ds\\&+\lim_{z\to\pm h_0}\frac{1}{2\pi}\sum_{j=4}^{6}\int_{-\infty}^{\infty}|s|\,p_{10j}^{(2)}d_{0j}^{T}(s,p)\exp\left[-|s|\gamma_{0j}(h_0-z)\right]\exp(-isx)ds\\&-\lim_{z\to\pm h_0}\frac{i}{2\pi}\sum_{j=1}^{2}\int_{-\infty}^{\infty}\frac{1}{s}p_{10j}^{(1)}F_{0j}(s,p)\exp\left[|s|(\tau h_{0j}+f_{0j}z)\right]\exp(isx)ds\end{aligned}\tag{52}$$

$$\begin{aligned}\sigma_{zx0}^{T*}(x,\pm h_0,p)&=\lim_{z\to\pm h_0}\frac{1}{2\pi}\sum_{j=1}^{3}\int_{-\infty}^{\infty}sp_{20j}^{(2)}d_{0j}^{T}(s,p)\exp\left[|s|\gamma_{oj}(h_0+z)\right]\exp(-isx)ds\\&+\lim_{z\to\pm h_0}\frac{i}{2\pi}\sum_{j=4}^{6}\int_{-\infty}^{\infty}sp_{20j}^{(2)}d_{0j}^{T}(s,p)\exp\left[-|s|\gamma_{0j}(h_0-z)\right]\exp(-isx)ds\\&-\lim_{z\to\pm h_0}\frac{i}{2\pi}\sum_{j=1}^{2}\int_{-\infty}^{\infty}\frac{1}{|s|}p_{20j}^{(1)}F_{0j}(s,p)\exp\left[|s|(\tau h_{0j}+f_{0j}z)\right]\exp(isx)ds\end{aligned}\tag{53}$$

$$\begin{aligned}D_{z0}^{T*}(x,\pm h_0,p)&=\lim_{z\to\pm h_0}\frac{1}{2\pi}\sum_{j=1}^{3}\int_{-\infty}^{\infty}|s|\,p_{30j}^{(2)}d_{0j}^{T}(s,p)\exp\left[|s|\gamma_{oj}(h_0+z)\right]\exp(-isx)ds\\&+\lim_{z\to\pm h_0}\frac{1}{2\pi}\sum_{j=4}^{6}\int_{-\infty}^{\infty}|s|\,p_{30j}^{(2)}d_{0j}^{T}(s,p)\exp\left[-|s|\gamma_{0j}(h_0-z)\right]\exp(-isx)ds\\&-\lim_{z\to\pm h_0}\frac{i}{2\pi}\sum_{j=1}^{2}\int_{-\infty}^{\infty}\frac{1}{s}p_{30j}^{(1)}F_{0j}(s,p)\exp\left[|s|(\tau h_{0j}+f_{0j}z)\right]\exp(isx)ds\end{aligned}\tag{54}$$

In Eqs. (52)-(54), the functions $d_{0j}^{T}(s,p)(j=1,2,\ldots,6)$ are also given in Appendix D. Of course, these components are superficial quantities and have no physical meaning in this analysis. However, they are equivalent to the crack face tractions in solving the crack problem by a proper superposition. The singular integral equations (45)-(50) are to be solved with the following subsidiary conditions obtained from the second boundary conditions (9)-(11).

$$\int_{a_k}^{b_k}G_{km}(\xi,p)d\xi=0\quad(k=1,2,m=1,2,3)\tag{55}$$

To solve the system of the singular integral equations (29), (30) and (45)-(50) with the subsidiary conditions (35), (55), we introduce the following functions $\Phi_{km}(\xi,p)(k=1,2,m=0,1,2,3)$:

$$G_{km}(\xi,p)=\frac{c_k}{[(a_k-|\xi|)(|\xi|-b_k)]^{1/2}}\Phi_{km}(\xi,p)\quad(k=1,2,m=0,1,2,3)\tag{56}$$

Using the Gauss-Jacobi integration formula [22], the functions $\Phi_{km}(\xi,p)$ (k = 1,2, m = 0,1,2,3) can be determined by solving the integral equations.

The stress intensity factors $K_{\mathrm{IA}}^{(k)*}(p)$, $K_{\mathrm{IB}}^{(k)*}(p)$, $K_{\mathrm{IIA}}^{(k)*}(p)$, $K_{\mathrm{IIB}}^{(k)*}(p)$ and the electric displacement intensity factors $K_{\mathrm{DA}}^{(k)*}(p)$, $K_{\mathrm{DB}}^{(k)*}(p)$ at the crack tips $x=a_k,b_k$ on the z = θ_{0k} (k = 1,2) planes in the Laplace transform plane may be, respectively defined and evaluated as:

$$\left.\begin{aligned}K_{\mathrm{IA}}^{(k)*}(p)&=-\lim_{x\to a_k}[2\pi(a_k-x)]^{1/2}\sigma_{zz0}^{*}(x,\theta_{0k},p)\\&=-(\pi c_k)^{1/2}\left[Z_{1k11}^{\infty}\Phi_{k1}(a_k,p)+Z_{1k31}^{\infty}\Phi_{k3}(a_k,p)\right]\\K_{\mathrm{IIA}}^{(k)*}(p)&=-\lim_{x\to a_k}[2\pi(a_k-x)]^{1/2}\sigma_{zx0}^{*}(x,\theta_{0k},p)\\&=-(\pi c_k)^{1/2}Z_{2k21}^{\infty}\Phi_{k2}(a_k,p)\\K_{\mathrm{DA}}^{(k)*}(p)&=-\lim_{x\to a_k}[2\pi(a_k-x)]^{1/2}D_{z0}^{*}(x,\theta_{0k},p)\\&=-(\pi c_k)^{1/2}\left[Z_{3k11}^{\infty}\Phi_{k1}(a_k,p)+Z_{3k31}^{\infty}\Phi_{k3}(a_k,p)\right]\end{aligned}\right\}\ (k=1,2)\tag{57}$$

$$\left.\begin{aligned}K_{\mathrm{IB}}^{(k)*}(p)&=\lim_{x\to b_k^{+}}[2\pi(x-b_k)]^{1/2}\sigma_{zz0}^{*}(x,\theta_{0k},p)\\&=(\pi c_k)^{1/2}\left[Z_{1k11}^{\infty}\Phi_{k1}(b_k,p)+Z_{1k31}^{\infty}\Phi_{k3}(b_k,p)\right]\\K_{\mathrm{IIB}}^{(k)*}(p)&=\lim_{x\to b_k^{+}}[2\pi(x-b_k)]^{1/2}\sigma_{zx0}^{*}(x,\theta_{0k},p)\\&=(\pi c_k)^{1/2}Z_{2k21}^{\infty}\Phi_{k2}(b_k,p)\\K_{\mathrm{DB}}^{(k)*}(p)&=\lim_{x\to b_k^{+}}[2\pi(x-b_k)]^{1/2}D_{z0}^{*}(x,\theta_{0k},p)\\&=(\pi c_k)^{1/2}\left[Z_{3k11}^{\infty}\Phi_{k1}(b_k,p)+Z_{3k31}^{\infty}\Phi_{k3}(b_k,p)\right]\end{aligned}\right\}\ (k=1,2)\tag{58}$$

Thus, the stress intensity factors $K_{\mathrm{IA}}^{(k)}(t)$, $K_{\mathrm{IB}}^{(k)}(t)$, $K_{\mathrm{IIA}}^{(k)}(t)$, $K_{\mathrm{IIB}}^{(k)}(t)$ and the electric displacement intensity factors $K_{\mathrm{DA}}^{(k)}(t)$, $K_{\mathrm{DB}}^{(k)}(t)$ (k = 1, 2) in the time-domain are

$$\left.\begin{aligned}K_{\mathrm{IA}}^{(k)}(t)&=-(\pi c_k)^{1/2}\frac{1}{2\pi i}\int_{Br}\left[Z_{1k11}^{\infty}\Phi_{k1}(a_k,p)+Z_{1k31}^{\infty}\Phi_{k3}(a_k,p)\right]\exp(pt)dp\\K_{\mathrm{IIA}}^{(k)}(t)&=-(\pi c_k)^{1/2}\frac{1}{2\pi i}\int_{Br}Z_{2k21}^{\infty}\Phi_{k2}(a_k,p)\exp(pt)dp\\K_{\mathrm{DA}}^{(k)}(t)&=-(\pi c_k)^{1/2}\frac{1}{2\pi i}\int_{Br}\left[Z_{3k11}^{\infty}\Phi_{k1}(a_k,p)+Z_{3k31}^{\infty}\Phi_{k3}(a_k,p)\right]\exp(pt)dp\end{aligned}\right\}(k=1,2)\tag{59}$$

$$\left.\begin{aligned}K_{\mathrm{IB}}^{(k)}(t)&=(\pi c_k)^{1/2}\frac{1}{2\pi i}\int_{Br}\left[Z_{1k11}^{\infty}\Phi_{k1}(b_k,p)+Z_{1k31}^{\infty}\Phi_{k3}(b_k,p)\right]\exp(pt)dp\\K_{\mathrm{IIB}}^{(k)}(t)&=(\pi c_k)^{1/2}\frac{1}{2\pi i}\int_{Br}Z_{2k21}^{\infty}\Phi_{k2}(b_k,p)\exp(pt)dp\\K_{\mathrm{DB}}^{(k)}(t)&=(\pi c_k)^{1/2}\frac{1}{2\pi i}\int_{Br}\left[Z_{3k11}^{\infty}\Phi_{k1}(b_k,p)+Z_{3k31}^{\infty}\Phi_{k3}(b_k,p)\right]\exp(pt)dp\end{aligned}\right\}(k=1,2)\tag{60}$$

The values of them at $t\to\infty$ are given by

$$\left.\begin{aligned}K_{\mathrm{IA}}^{(k)}(\infty)&\equiv\lim_{t\to\infty}K_{\mathrm{IA}}^{(k)}(t)=\lim_{p\to0}pK_{\mathrm{IA}}^{(k)*}(p)\\K_{\mathrm{IIA}}^{(k)}(\infty)&\equiv\lim_{t\to\infty}K_{\mathrm{IIA}}^{(k)}(t)=\lim_{p\to0}pK_{\mathrm{IIA}}^{(k)*}(p)\\K_{\mathrm{DA}}^{(k)}(\infty)&\equiv\lim_{t\to\infty}K_{\mathrm{DA}}^{(k)}(t)=\lim_{p\to0}pK_{\mathrm{DA}}^{(k)*}(p)\end{aligned}\right\}\quad(k=1,2)\tag{61}$$

$$\left.\begin{aligned}K_{\mathrm{IB}}^{(k)}(\infty)&\equiv\lim_{t\to\infty}K_{\mathrm{IB}}^{(k)}(t)=\lim_{p\to}pK_{\mathrm{IB}}^{(k)}(p)\\K_{\mathrm{IIB}}^{(k)}(\infty)&\equiv\lim_{t\to\infty}K_{\mathrm{IIB}}^{(k)}(t)=\lim_{p\to}pK_{\mathrm{IIB}}^{(k)}(p)\\K_{\mathrm{DB}}^{(k)}(\infty)&\equiv\lim_{t\to\infty}K_{\mathrm{DB}}^{(k)}(t)=\lim_{p\to}pK_{\mathrm{DB}}^{(k)}(p)\end{aligned}\right\}\quad(k=1,2)\tag{62}$$

Numerical Results and Discussion

For the numerical calculations, the material is considered to be cadmium selenide, with the following properties [2] are used properties of the FGPM plate at the plane z = 0:

$$\left.\begin{array}{ll} c_{110}=7.41\times10^{10}[\mathrm{N/m^2}], & c_{130}=3.93\times10^{10}[\mathrm{N/m^2}], \\ c_{330}=8.36\times10^{10}[\mathrm{N/m^2}], & c_{440}=1.32\times10^{10}[\mathrm{N/m^2}], \\ e_{310}=-0.16[\mathrm{C/m^2}], & e_{330}=0.347[\mathrm{C/m^2}], \\ e_{150}=-0.138[\mathrm{C/m^2}], & \\ \varepsilon_{110}=0.825\times10^{-10}[\mathrm{C/Vm}], & \varepsilon_{330}=0.903\times10^{-10}[\mathrm{C/Vm}], \\ \lambda_{110}=0.621\times10^{6}[\mathrm{N/Km^2}], & \lambda_{330}=0.551\times10^{6}[\mathrm{N/Km^2}], \\ p_{z0}=-2.94\times10^{-6}[\mathrm{C/Km^2}] & \end{array}\right\} \quad (63)$$

Since the values of the coefficients of heat conduction for cadmium selenide could not be found in the literature, the value $\kappa^2 = \kappa_x/\kappa_z = 1/1.5$ is assumed.

To examine the effects of the crack geometry and material parameters on $K_{\eta\mathrm{A}}^{(k)}$, $K_{\eta\mathrm{B}}^{(k)}$ $(\eta=\mathrm{I},\mathrm{II},\mathrm{D},k=1,2)$, the normalized parameters ($c_1/h, c_2/h, h_0/h, h_1/h, h_2/h, d/h$ and (βh, δh, ωh) are used. Because there are many geometric parameters, we focus on the influence of the crack distance parameter d/h and the material non-homogeneity on the fracture behavior. Thus it is supposed to be the crack location parameters $h_1/h = h_2/h = 0.5$ and the crack length parameters $c_1/h = c_2/h$. And the normalized non-homogeneous parameters βh, δh and ωh are assumed to be $\beta h = \delta h = \omega h$.

The electroelastic fields without cracks

Figures 2a-2c indicate the normalized stress components $(\sigma_{zz0}^T(x,\pm h_0,t),\ \sigma_{zx0}^T(x,\pm h_0,t))/\lambda_{330}T_0$ and the normalized electric displacement component $D_{z0}^T(x,\pm h_0,t)/p_{z0}T_0$ on the $z/h=\pm0.2$ planes in the strip without crack at various normalized time $F=t\lambda_0/h^2$ for the crack distance parameter d/h = 1.5, the crack spacing parameter h_0/h = 0.2, the crack length parameter $c_1/h = c_2/h = 1.0$ and βh = 1.0. Above mentioned before, these components are given by Eqs. (52)-(54) and are superficial quantities. The maximum values of $\sigma_{zz0}^T(x,h_0,t)$, $\sigma_{zx0}^T(x,h_0,t)$ and $D_{z0}^T(x,h_0,t)$ are seen to occur at about $F\approx0.5$, whereas the maximum values of $\sigma_{zz0}^T(x,-h_0,t)$, $\sigma_{zx0}^T(x,-h_0,t)$ and $D_{z0}^T(x,-h_0,t)$ occur at F→∞.

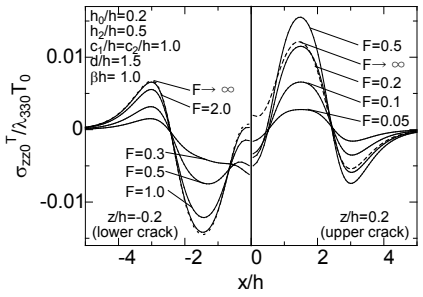

Figure 2a: The stress component σ_{zz0}^T on the *z/h* = ± 0.2 planes in the strip without crack.

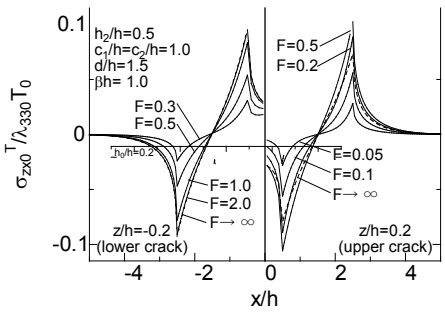

Figure 2b: The stress component σ_{zx}^T on the *z/h* = ± 0.2 planes in the strip without crack.

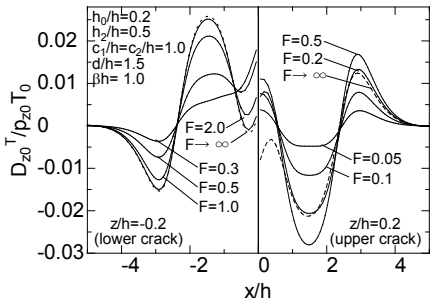

Figure 2c: The electric displacement component D_{z0}^T on the *z/h* = ± 0.2 planes in the strip without crack.

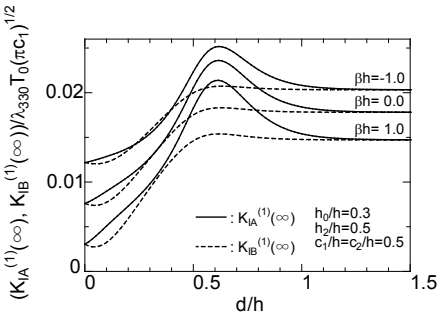

Figure 3a: The effects of the material non-homogeneity and the crack distanceon the static values of the stress intensity factors $K_{\mathrm{IA}}^{(1)}(\infty)$ and $K_{\mathrm{IB}}^{(1)}(\infty)$.

The static behavior of the stress and electric displacement intensity factors

Due to above discussion, the intensity factors of the upper crack would be larger than those of the lower crack, thus only the results for the upper crack will be shown. Figures 3a-3c show the effects of the material non-homogeneity βh and the crack distance d/h on the static values of the normalized stress intensity factors $(K_{\eta\mathrm{A}}^{(1)}(\infty), K_{\eta\mathrm{B}}^{(1)}(\infty))/\lambda_{330}T_0(\pi c)^{1/2}$ $(\eta=\mathrm{I},\mathrm{II})$ and the static values of the normalized electric displacement intensity factors $(K_{\mathrm{DA}}^{(1)}(\infty), K_{\mathrm{DB}}^{(1)}(\infty))/p_{z0}T_0(\pi c)^{1/2}$ for βh = -1.0,0.0,1.0 with h_0/h = 0.3 and $c_1/h = c_2/h$ = 0.5. The results for the cases of $d/h\to\infty$ and βh = 0.0 coincide with the results of single parallel crack [8] and with the results for the homogeneous case [14], respectively. The values of the intensity factors tend to increase/decrease at first, reach maximum/minimal values and then decrease/increase with increasing d/h. The absolute maximum values of the intensity factors tend to occur at about $c_1/h = d/h$, and the interaction between the two cracks may vanish for the range $3c_1/h<d/h$. Moreover, it is evident that the intensity factors can be reduced by increasing the material property gradient of functionally graded piezoelectric materials.

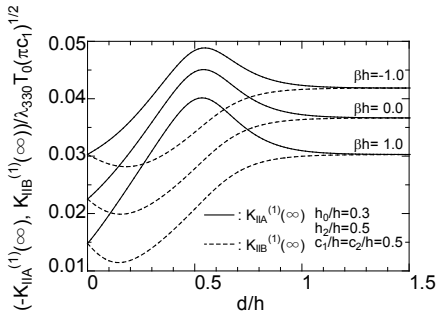

Figure 3b: The effects of the material non-homogeneity and the crack distance d on the static values of the stress intensity factors $K_{\mathrm{IIA}}^{(1)}(\infty)$ and $K_{\mathrm{IIB}}^{(1)}(\infty)$.

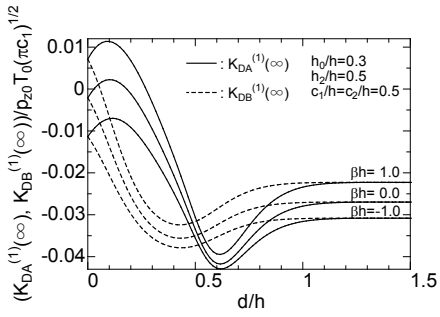

Figure 3c: The effects of the material non-homogeneity and the crack distance d on the static values of the electric displacement intensity factors $K_{\mathrm{DA}}^{(1)}(\infty)$ and $K_{\mathrm{DB}}^{(1)}(\infty)$.

The transient behavior of the stress and electric displacement intensity factors

Figures 4a-4c show the effect of the crack distance d/h on the transient behavior of the normalized stress intensity factors $(K_{\eta\mathrm{A}}^{(1)}, K_{\eta\mathrm{B}}^{(1)})/\lambda_{330}T_0(\pi c)^{1/2}(\eta=\mathrm{I},\mathrm{II})$ and the normalized electric displacement intensity factors $(K_{\mathrm{DA}}^{(1)}, K_{\mathrm{DB}}^{(1)})/p_{z0}T_0(\pi c)^{1/2}$ are plotted versus F for βh = 1.0 with h_0/h = 0.2 and $c_1/h = c_2/h$ = 1.0. In these figures, the dashed, solid and dotted lines indicate the results for d/h = 0.5,1.0 and 3.0, respectively.

Similar to the static values of the normalized stress and electric displacement intensity factors, the interaction between the two cracks may vanish for $3c_1/h = d/h$, and the absolute values of the intensity factors become $|K_{\eta\mathrm{A}}^{(1)}| = |K_{\eta\mathrm{B}}^{(1)}|\ (\eta=\mathrm{I},\mathrm{II},\mathrm{D})$. The absolute values of the intensity factors $|K_{\eta\mathrm{A}}^{(1)}|$, $|K_{\eta\mathrm{B}}^{(1)}|\ (\eta=\mathrm{I},\mathrm{II},\mathrm{D})$ increase at first, have the peak values $|K_{\eta\mathrm{A}}^{(1)peak}|$, $|K_{\eta\mathrm{B}}^{(1)peak}|\ (\eta=\mathrm{I},\mathrm{II},\mathrm{D})$, then decrease and approach the static values $|K_{\eta\mathrm{A}}^{(1)}(\infty)|$, $|K_{\eta\mathrm{B}}^{(1)}(\infty)|\ (\eta=\mathrm{I},\mathrm{II},\mathrm{D})$ with increasing F. The value of $K_{\mathrm{IA}}^{(1)}$ (d/h = 0.5) becomes negative so that the contact of the crack faces would occur, and these results for F >1.3 have no physical meaning. As shown in the previous paper [18], the results presented here without considering this effect may not be exactly correct but would be more conservative, since the contact of the crack faces will increase the friction between the faces and make heat and electric transfer across the crack faces easier. Thus the intensity factors would be lowered by these two factors.

Figures 5a-5c show the effect of the material non-homogeneity βh on $(K_{\eta\mathrm{A}}^{(1)}, K_{\eta\mathrm{B}}^{(1)})/\lambda_{330}T_0(\pi c)^{1/2}(\eta=\mathrm{I},\mathrm{II})$ and $(K_{\mathrm{DA}}^{(1)}, K_{\mathrm{DB}}^{(1)})/p_{z0}T_0(\pi c)^{1/2}$ are plotted versus F for d/h = 0.0 with $c_1/h = c_2/h$ = 1.0. In these figures, the solid, dotted and dashed lines indicate the results for βh = 2.0, 0.0 and -2.0, respectively. The results for the case of βh = 0.0 coincident with two parallel cracks [17] and with the results for the homogeneous case [18]. Because of symmetry, the values of $K_{\eta\mathrm{A}}^{(1)}$, $K_{\eta\mathrm{B}}^{(1)}(\eta=\mathrm{I},\mathrm{D})$ for βh = 0.0 approach zero and the values of the intensity factors are $K_{\eta\mathrm{A}}^{(1)} = K_{\eta\mathrm{B}}^{(1)}(\eta=\mathrm{I},\mathrm{D})$ and $K_{\mathrm{IIA}}^{(1)} = -K_{\mathrm{IIB}}^{(1)}$. The value of $K_{\mathrm{IA}}^{(1)}$ for βh = 2.0 also becomes negative so that the contact of the crack faces would occur.

Figures 6a-6c are the same as Figures 5a-5c for d/h = 1.0. With

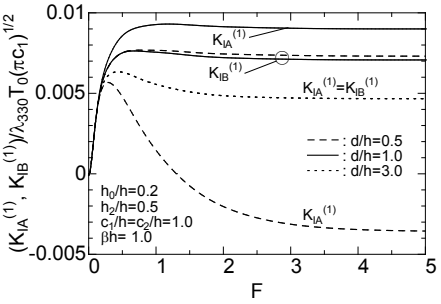

Figure 4a: The effect of the crack distance d on the stress intensity factors $K_{\mathrm{IA}}^{(1)}$ and $K_{\mathrm{IB}}^{(1)}$.

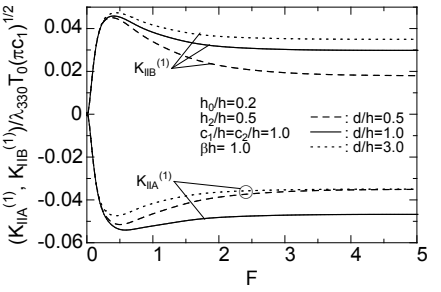

Figure 4b: The effect of the crack distance d on the stress intensity factors $K_{\mathrm{IIA}}^{(1)}$ and $K_{\mathrm{IIB}}^{(1)}$.

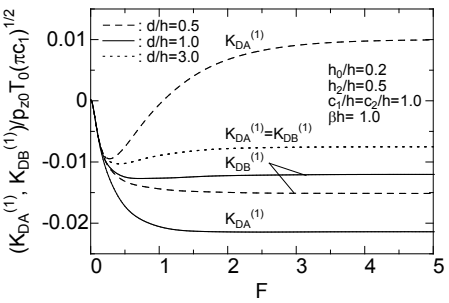

Figure 4c: The effect of the crack distance d on the electric displacement intensity factors $K_{\mathrm{DA}}^{(1)}$ and $K_{\mathrm{DB}}^{(1)}$.

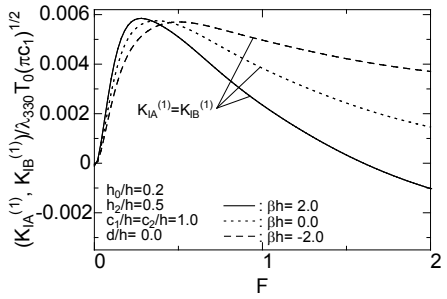

Figure 5a: The effect of the material non-homogeneity on the stress intensity factors $K_{IA}^{(1)}$ and $K_{IB}^{(1)}$ for d/h = 0.0 and βh = 2.0,0.0, -2.0.

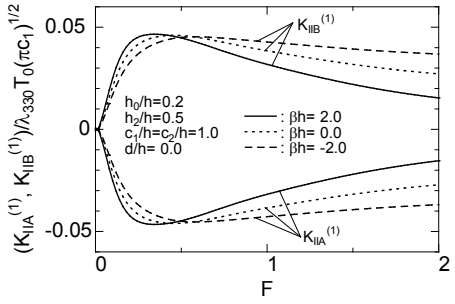

Figure 5b: The effect of the material non-homogeneity on the stress intensity factors $K_{IIA}^{(1)}$ and $K_{IIB}^{(1)}$ for d/h = 0.0 and βh = 2.0,0.0, -2.0

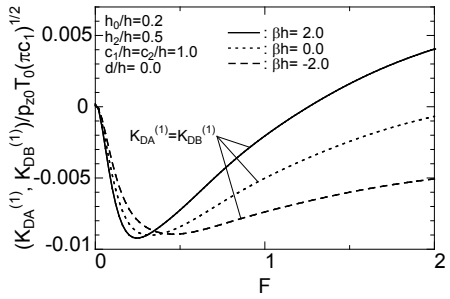

Figure 5c: The effect of the material non-homogeneity on the electric displacement intensity factors $K_{DA}^{(1)}$ and $K_{DB}^{(1)}$ d/h = 0.0 and βh = 2.0,0.0, -2.0.

increasing F, the intensity factors $K_{\eta A}^{(1)}$, $K_{\eta B}^{(1)}(\eta = \mathrm{I,D})$ and $K_{IIA}^{(1)}$ for βh = -2.0 increase monotonically, and then approach static values $K_{\eta A}^{(1)}(\infty)$, $K_{\eta B}^{(1)}(\infty)(\eta = \mathrm{I,D})$ and $K_{IIA}^{(1)}(\infty)$. On the other hand, the intensity factors $K_{\eta A}^{(1)}$, $K_{\eta B}^{(1)}(\eta = \mathrm{I,II})$ and $K_{DB}^{(1)}$ for $\beta h = 2.0$ have clear peak values, and $K_{IA}^{(1)}$, $K_{IB}^{(1)}$ for $\beta h = 0.0$ have slight peak values. In addition, these peak values, static values and the interesting values $(|K_{\eta A}^{(1)peak} - K_{\eta A}^{(1)}(\infty)|)/|K_{\eta A}^{(1)}(\infty)|$, $(|K_{\eta B}^{(1)peak} - K_{\eta B}^{(1)}(\infty)|)/|K_{\eta B}^{(1)}(\infty)|(\eta = \mathrm{I,II,D})$, which mean the overshooting effect, are presented in Tables 1-3. It is found that the peak values of the intensity factors and the overshooting effects increase with increasing βh.

Conclusion

The transient mixed-mode thermoelectroelastic fracture problem of a functionally graded piezoelectric material strip with two parallel cracks in arbitrary positions is studied theoretically. For the special cases of symmetrical geometry ($h_1/h = h_2/h = 0.5$ and $c_1/h = c_2/h$), the effects of the crack distance and material non-homogeneity on the stress and electric displacement intensity factors are clarified. The following facts can be found from the numerical results.

For the case of the static behavior

1. The increase of the material parameter is beneficial for reducing the static values of the intensity factors.

2. The absolute maximum values of the intensity factors tend to occur at about $c_1/h = d/h$, and the interaction between the two cracks becomes 0 at about $3c_1/h = d/h$.

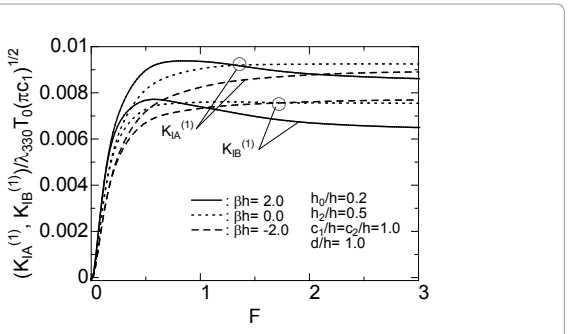

Figure 6a: The effect of the material non-homogeneity on the stress intensity factors $K_{IA}^{(1)}$ and $K_{IB}^{(1)}$ for d/h = 1.0 and βh = 2.0,0.0, -2.0.

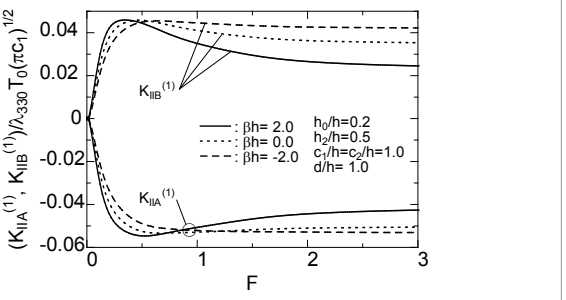

Figure 6b: The effect of the material non-homogeneity on the stress intensity factors $K_{IIA}^{(1)}$ and $K_{IIB}^{(1)}$ for d/h = 1.0 and βh = 2.0,0.0, -2.0.

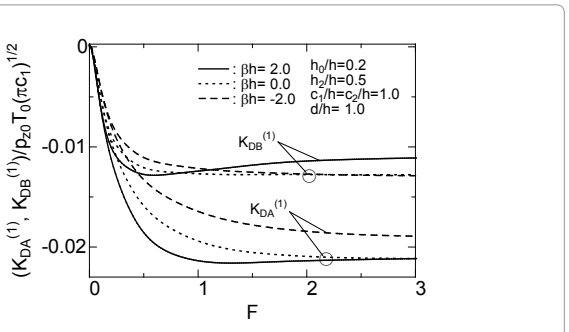

Figure 6c: The effect of the material non-homogeneity on the electric displacement intensity factors $K_{DA}^{(1)}$ and $K_{DB}^{(1)}$ for d/h = 1.0 and βh = 2.0,0.0, -2.0.

Figure	*k*	*d*/*h*	*βh*	$\frac{\lvert K_{Ik}^{peak}\rvert}{\lambda_{330}T_0(\pi c_1)^{1/2}}$	$\frac{\lvert K_{Ik}(\infty)\rvert}{\lambda_{330}T_0(\pi c_1)^{1/2}}$	$\frac{\lvert K_{Ik}^{peak}-K_{Ik}(\infty)\rvert}{\lvert K_{Ik}(\infty)\rvert}$
			2.0	9.383 × 10^{-3}	8.616 × 10^{-3}	0.089
Figure 6a	A	1.0	0.0	9.254 × 10^{-3}	9.239 × 10^{-3}	0.002
			-2.0	8.906 × 10^{-3}	8.906 × 10^{-3}	0.000
			2.0	7.718 × 10^{-3}	6.498 × 10^{-3}	0.188
Figure 6a	B	1.0	0.0	7.611 × 10^{-3}	7.547 × 10^{-3}	0.008
			-2.0	7.691 × 10^{-3}	7.691 × 10^{-3}	0.000

Table 1: The values of $|K_{Ik}^{peak}|/\lambda_{330}T_0(\pi c_1)^{1/2}$, $|K_{Ik}(\infty)|/\lambda_{330}T_0(\pi c_1)^{1/2}$ and $(|K_{Ik}^{peak}-K_{Ik}(\infty)|)/|K_{Ik}(\infty)|$

Figure	*k*	*d*/*h*	*βh*	$\frac{\lvert K_{IIk}^{peak}\rvert}{\lambda_{330}T_0(\pi c_1)^{1/2}}$	$\frac{\lvert K_{IIk}(\infty)\rvert}{\lambda_{330}T_0(\pi c_1)^{1/2}}$	$\frac{\lvert K_{IIk}^{peak}-K_{IIk}(\infty)\rvert}{\lvert K_{IIk}(\infty)\rvert}$
			2.0	5.466 × 10^{-2}	4.263 × 10^{-2}	0.282
Figure 6b	A	1.0	0.0	5.340 × 10^{-2}	5.055 × 10^{-2}	0.056
			-2.0	5.308 × 10^{-2}	5.308 × 10^{-2}	0.000
			2.0	4.591 × 10^{-2}	2.455 × 10^{-2}	0.870
Figure 6b	B	1.0	0.0	4.582 × 10^{-2}	3.536 × 10^{-2}	0.296
			-2.0	4.553 × 10^{-2}	4.224 × 10^{-2}	0.078

Table 2: The values of $|K_{IIk}^{peak}|/\lambda_{330}T_0(\pi c_1)^{1/2}$, $|K_{IIk}(\infty)|/\lambda_{330}T_0(\pi c_1)^{1/2}$ and $(|K_{IIk}^{peak}-K_{IIk}(\infty)|)/|K_{IIk}(\infty)|$.

Figure	*k*	*d*/*h*	*βh*	$\frac{\lvert K_{Ik}^{peak}\rvert}{\lambda_{330}T_0(\pi c_1)^{1/2}}$	$\frac{\lvert K_{Ik}(\infty)\rvert}{\lambda_{330}T_0(\pi c_1)^{1/2}}$	$\frac{\lvert K_{Ik}^{peak}-K_{Ik}(\infty)\rvert}{\lvert K_{Ik}(\infty)\rvert}$
			2.0	2.161 × 10^{-2}	2.116 × 10^{-2}	0.021
Figure 6c	A	1.0	0.0	2.116 × 10^{-2}	2.116 × 10^{-2}	0.000
			-2.0	1.892 × 10^{-2}	1.892 × 10^{-2}	0.000
			2.0	1.283 × 10^{-2}	1.110 × 10^{-2}	0.156
Figure 6c	B	1.0	0.0	1.277 × 10^{-2}	1.277 × 10^{-2}	0.000
			-2.0	1.287 × 10^{-2}	1.287 × 10^{-2}	0.000

Table 3: The values of $|K_{Dk}^{peak}|/\lambda_{330}T_0(\pi c_1)^{1/2}$, $|K_{Dk}(\infty)|/\lambda_{330}T_0(\pi c_1)^{1/2}$ and $(|K_{Dk}^{peak}-K_{Dk}(\infty)|)/|K_{Dk}(\infty)|$.

For the case of the transient behavior

1. The distinct overshooting phenomenon can be observed and this fact may suggest the importance of these transient analyses.

2. The peak values of the intensity factors increase with increasing βh.

3. The overshooting effect depends on the crack distance and material non-homogeneity. The large βh induces the large overshooting effect.

References

1. Rao SS, Sunar M (1994) Piezoelectricity and its use in disturbance sensing and control of flexible structures: A survey. Applied Mechanics Review 47: 113-123.
2. Ashida F, Tauchert TR (1998) Transient response of a piezothermoelastic circular disk under axisymmetric heating. Acta Mechanica 128: 1-14.
3. Wu CM, Kahn M, Moy W (1996) Piezoelectric ceramics with functionally gradients: A new application in material design. J American Ceramics Society 79: 809-812.
4. Chen J, Liu ZX, Zou ZZ (2003) Electromechanical impact of a crack in a functionally graded piezoelectric medium theoretical and applied fracture mechanics 39: 47-60.
5. Wang BL, Zhang XH (2004) A mode III crack in functionally graded piezoelectric material strip transactions of the ASME. J Applied Mechanics 71: 327-333.
6. Ueda S (2006) A Finite crack in a semi-infinite strip of a grade piezoelectric material under electric loading. European J Mechanics A/Solids 25: 250-259.
7. Ueda S (2008) A cracked functionally graded piezoelectric material strip under transient thermal loading. Acta Mechanica 199: 53-70.
8. Ueda S (2007) Thermal intensity factors for a parallel crack in a functionally graded piezoelectric strip. J Thermal Stresses 30: 321-342.
9. Ueda S (2007) Effects of crack surface conductance on intensity factors for a cracked functionally graded piezoelectric material under thermal load. J Thermal Stresses 30: 731-752.
10. Ueda S (2007) A penny-shaped crack in a functionally graded piezoelectric strip under thermal loading. Engineering Fracture Mechanics 74: 1255-1273.
11. Ueda S (2008) Transient thermoelectroelastic response of a functionally graded piezoelectric strip with a penny-shaped crack. Engineering Fracture Mechanics 75: 1204-1222.
12. Ueda S, Nishimura N (2008) An annular crack in a functionally graded piezoelectric strip under thermoelectric loadings. J Thermal Stresses 31: 1079-1098.
13. Ueda S, Tani Y (2008) Thermal stress intensity factors for two coplanar cracks in a piezoelectric strip. Journal of Thermal Stresses 31: 403-415.
14. Ueda S, Nishikohri H (2013) Two parallel cracks in arbitrary positions of a piezoelectric material strip under thermo-electric loadings. J Thermal Stresses 36: 480-500.
15. Ueda S, Uemura Y (2009) Thermoelectromechanical interaction among multi parallel cracks in a piezoelectric Material. J Thermal Stresses 32: 1005-1023.
16. Ueda S, Hatano H (2012) T-Shaped crack in a piezoelectric material thermo-electro-mechanical loadings. J Thermal Stresses 35: 12-29.

17. Ueda S, Ikeda Y, Ishii A (2012) Transient thermoelectromechanical response of a piezoelectric strip with two parallel cracks of different lengths. J Thermal Stresses 35: 534-549.

18. Ueda S, Nishikohri H (2016) Transient thermoelectroelastic response of a piezoelectric material Strip with two parallel cracks in arbitrary positions. J Thermal Stresses in press.

19. Ueda S, Iogawa T (2010) Two parallel penny-shaped or annular cracks in a functionally graded piezoelectric strip under electric loading. Acta Mechanica 210: 57-70.

20. Ueda S, Ueda T (2013) Transient thermoelectroelastic response of a functionally graded piezoelectric strip with two parallel Axisymmetric Cracks. J Thermal Stresses 36: 1027-1055.

21. Sneddon IN, Lowengrub M (1969) Crack Problems in the classical theory of elasticity John Wiley and Sons Inc New York.

22. Erdogan F, Wu BH (1996) Crack problems in FGM Layers under thermal stresses. J Thermal Stresses 19: 237-265.

23. Erdogan F, Gupta GD, Cook TS (1972) Methods of analysis and solution of crack problems in GC Sih (edn) Noordhoff Leyden.

24. Miller MK, Guy WT (1966) Numerical inversion of the laplace transform by use of jacobi polynomials. SIAM J Numerical Analysis 3: 624-635.

25. Wang BL, Mai YW (2004) Impermeable crack and permeable crack assumptions which one is more realistic? transactions of the ASME J Applied Mechanics 71: 575-578.